Hindawi Publishing Corporation
EURASIP Journal on Wireless Communications and Networking
Volume 2008, Article ID 732145, 13 pages
doi:10.1155/2008/732145

Research Article

Energy Efficiency Comparison of MIMO-Based and Multihop Sensor Networks

George Bravos and Athanasios G. Kanatas

Wireless Communications Laboratory, Department of Technology Education and Digital Systems, University of Piraeus, 80 Karaoli and Dimitriou Street, 18534 Piraeus, Greece

Correspondence should be addressed to George Bravos, gebravos@unipi.gr

Received 11 July 2007; Revised 16 October 2007; Accepted 12 December 2007

Recommended by Richard Kozick

Wireless sensor networks (WSNs) demand the implementation of energy-aware techniques and low-complexity protocols in all layers. Recently, a MIMO-based structure has been proposed to offer enhanced energy savings in WSNs. In this paper, we examine and compare MIMO-based WSN with a multihop transmission in terms of energy efficiency. The results depend on the network density, the channel conditions, and the distance to the destination node. We reach analytical expressions to calculate threshold values of these parameters, which determine the areas where the MIMO-based structure outperforms multihop transmission. Moreover, we present a detailed analysis of the dissipated power during a sensor node_s operation, to prove that as microelectronics develops, the MIMO-based architecture will outperform the equivalent multihop structure for most of the cases examined. Finally, we implement a simple cooperative node selection algorithm to achieve higher energy gains in the MIMO approach, and we examine how this algorithm affects the calculated thresholds.

1. INTRODUCTION

One of the most important characteristics of a WSN is that the sensor nodes usually operate on small batteries, which are difficult to replace, and thus have restricted sources of energy [1]. Consequently, the design of such networks should focus primarily on improving the performance in terms of energy efficiency.

A technique that has been recently introduced in WSNs focusing on energy efficiency is cooperative networking. A sensor network may be seen as a multi-input/multioutput (MIMO) system, where a sensor node is assigned the role of a transmitting or receiving antenna of the MIMO structure. This structure may offer enhanced energy gains for a WSN, depending on the distance between the Tx and Rx sides of the system.In [2], it was proved that a MIMO system supports higher data rates without increasing transmission power, which is equivalent to the conclusion that MIMO systems demand less transmission energy than single-input/single-output (SISO) systems for the same throughput requirements. This view was used in [3], where the authors proved that under certain conditions a sensor network may operate based on a MIMO structure. Moreover, there is a critical distance between the transmitter and the receiver above which MIMO transmission is more energy-efficient than SISO. This topic was furtherly discussed in [4], where a thorough study towards the energy efficiency of MIMO-based schemes was carried out.

A very interesting extension of the work on MIMO-based WSNs is an architecture called MIMO-sensor networks with mobile agents (M-SEMNA), proposed in [5]. According to M-SEMNA, several neighboring nodes are selected to transmit information cooperatively, whereas the data sink is equipped with multiple antennas. Such receiver though does not suffer from energy limitations; thus the results obtained, however promising they are, are not applicable to several WSN applications. In [6], the proposed protocol is based on extending the traditional low-energy adaptive clustering hierarchy protocol (LEACH) by incorporating the cooperative MIMO communication.

Introducing a MIMO structure in a wireless sensor network raises several issues. One of them is the implementation of cooperative techniques, for example, cooperative node selection, for energy-efficient operation. The selection of the

nodes that form the virtual antenna array in order to transmit the data seriously affects the network's energy consumption. In [7], a new MAC protocol based on cooperation is proposed. No specific relay algorithm is defined though. An interesting scheme is proposed in [8] including two different policies for selecting the best relay node, based mainly on channel estimates. Finally, an algorithm that considers also the remaining energy of the neighbor nodes before choosing the cooperation node may be found in [6].

Although several comparisons regarding energy consumption have been made between MIMO-based and simple SISO-based networks, no comparison has been made—to our knowledge—versus the energy consumed by a network based on multihop transmission. One of the contributions of this paper is the investigation of the parameters that affect the energy efficiency of a MIMO-based sensor network in comparison to a SISO multihop-based network. In particular, we focus on the distance between the transmitter and the receiver, the node density, and the channel conditions. Moreover, we estimate the threshold values over which the MIMO structure is more energy-efficient. Two cases of multihop networks are investigated regarding the transmission range of the nodes. On the first one, a typical range value is used, while on the second one an optimization algorithm is applied.

Considering the rapid technology evolution, we elaborate on the results using three different examined scenarios regarding the electronics used in the hardware and the power they dissipate. In addition, we implement a simple but very effective cooperative node selection algorithm, and estimate its effect on the threshold values of the examined parameters. For both cases, we prove that as technology develops, the thresholds that determine MIMO structure's energy efficiency become looser, and in the short future MIMO transmissions should be applied in WSNs for most cases.

The remainder of the paper is organized as follows. Section 2 presents a brief description of the MIMO and multihop structures on sensor networks, along with the models used for energy consumption and distances between nodes in the network. The energy estimation analysis is done in Section 3, followed by threshold values estimations and future tendencies that are gathered and marked upon in Section 4. Section 5 describes the cooperation node selection algorithm and its effect on the estimated thresholds. Finally, a summary is made in Section 6, along with some useful conclusions.

2. SISO AND MIMO MULTIHOP APPROACH: MODELING ENERGY AND SPACE

2.1. SISO and MIMO-based transmission

The most common communication way in WSNs is to forward the data through multiple hops, using intermediate nodes that are deployed between the source and the destination. Let H_{multi} denote the total number of hops needed for the data to reach the destination node, and let E_b be the energy consumed for transmitting one bit of data at each hop.

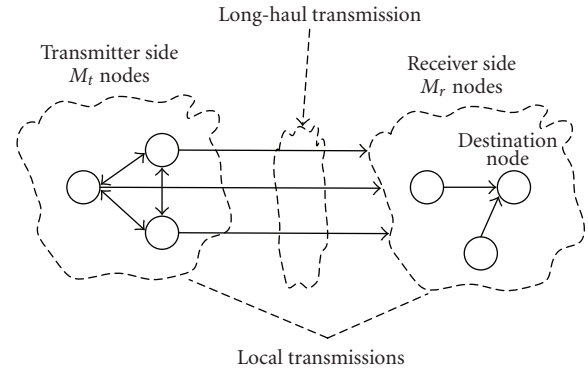

Figure 1: MIMO-based approach for WSNs.

Then, the total energy consumption for transmitting L bits of data from a source to a destination node is given by

$$E_{\text{multihop}} = H_{\text{multi}} L E_b. \tag{1}$$

On the other hand, the basic idea in the MIMO-based structure for WSNs is that there are M_t neighbor nodes with data to be transmitted to a destination node. Each node broadcasts its information to all neighbor nodes using different time slots (local transmissions), and in what follows, the transmission sequence is encoded according, for example, to the Alamouti diversity codes [2]. The ith node then transmits the sequence that the ith antenna would transmit in an Alamouti MIMO system (long-haul transmission). On the receiver side, the M_r nodes, with the destination node included, receive the encoded data, and the $M_r - 1$ nodes forward the data to the destination node after quantizing each symbol into n_r bits. The MIMO approach is explained in [3] and summarized in Figure 1.

The energy required to complete a transmission of L bits based on this MIMO structure is given by [3]

$$E_{\text{MIMO}} = L_{\text{MIMO}} \sum_{i=1}^{M_t} E_{b,i}^t + L_{\text{MIMO}}\, E_b^l M_t + \frac{(L_{\text{MIMO}} M_t)}{b} \sum_{j=1}^{M_r - 1} E_{b,j}^r n_r, \tag{2}$$

where E_b^t, E_b^r, E_b^l are the energy consumptions for transmitting and receiving one bit of data in the transmitter side and the receiver side and for the long-haul transmission, respectively, and $L_{\text{MIMO}} = L/M_t$. In general, E_b is a function of the path loss factor n and the average range of the nodes d. In the case of local transmissions, the range depends on the distance between two neighbouring nodes, d_k. For long-haul transmissions, we use the average distance between source and destination nodes, denoted by D. We assume that channel conditions are approximately the same at both the receiver side and the transmitter side; so the value of the path loss factor n is the same for all cases. Finally, $(L_{\text{MIMO}} M_t)/b$ expresses the total number of symbols transmitted from the transmitter's side, assuming that b is the constellation size used by the Alamouti code.

Table 1: Typical values of energy model parameters.

a	1.33
P_{syn}	25 mW
P_c	22.9 mW
T_{tr}	5 μs
P_{detector}	5 mW

2.2. Energy model

The energy (E_b) consumed to transmit and receive one bit is expressed by

$$E_b = \frac{\left(P_t + aP_t + P_c + P_{\text{detector}}\right) T_{\text{on}} + 2P_{\text{syn}} T_{\text{tr}}}{L}. \tag{3}$$

In (3), a expresses the energy consumption in the power amplifier and depends on the modulation used [9, 10], T_{tr} is the transition time needed for the node to change from the "sleep" to the "awake" mode, and P_{syn}, P_{detector}, P_c represent the power dissipated in the frequency synthesizers, the detector, and the rest of the circuitry. T_{on} is the time needed for the transmission of L bits, depending on the transmission rate R_b ($T_{\text{on}} = L/R_b$), and P_t is the transmitted power calculated by the link budget equation [11]

$$P_t(d,n)_{(\text{dBW})} = \overline{PL(d,n)}_{(\text{dB})} + \frac{E_{b,\text{required}}}{N_{0(\text{dB})} + R_{b(\text{dBHz})} - 204_{(\text{dBW/Hz})} + S_{(\text{dB})}}, \tag{4}$$

where $\overline{PL}$ is the average path loss accounting for large-scale fading, S is a safety margin, -204 dBW/Hz is a typical value of N_0, and $E_{b,\text{required}}/N_0$ depends on the channel, the modulation used, and the target BER [12]. The average path loss is calculated by a single slope model. Typical values for the parameters used in the energy model are shown in Table 1. More details on the complete energy model used to estimate E_b can be found in [9].

2.3. Space model

Assume that M sensor nodes are randomly deployed in a square surface with length $2R$ on each edge. Using a two-dimensional Poisson distribution model [13], the distance between two neighboring nodes, defined as d_k, is a random variable (r.v.) with a mean value that is expressed with the help of node density ρ_s as [13]

$$E[d_k] = \overline{d_k} = \sqrt{\frac{1}{4\rho_s}} = \frac{R}{\sqrt{M}}, \qquad \rho_s = \frac{M}{4R^2}. \tag{5}$$

During the sensor network's operation, a node called *source node* senses a piece of data and has to deliver it to the *destination node*, which may be any of the M nodes of the network. The distance between *source node* and *destination node*, denoted by D, is also an r.v. that according to [13, 14], has a mean value given by

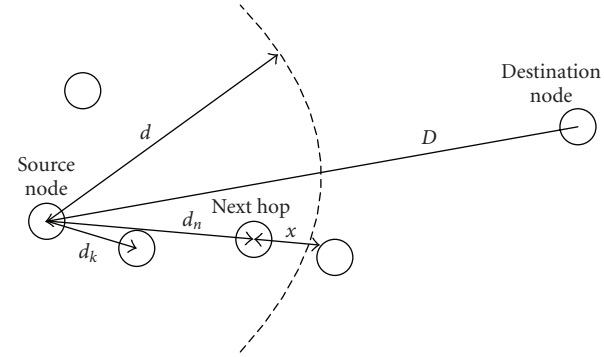

Figure 2: Space modeling.

$$E[D] = \overline{D} = \frac{R}{3}\left[\sqrt{2} + \ln\left(1 + \sqrt{2}\right)\right]. \tag{6}$$

The last variable that has to be modeled is the distance between the *source node* and the *next hop*, which is used in the case of multihop transmission and is denoted by d_n. The *next hop* is in the direction of the destination node, and it is selected to be the closest node to the range d of the *source*. In order to model d_n, we model the distance x between the range limits (d) and the *next hop*. Hence,

$$\overline{d_n} = d - \overline{x}. \tag{7}$$

Using the two-dimensional Poisson model, we estimate the mean value of x by

$$E[x] = \overline{x} \simeq \frac{1}{\left(4\rho_s + 1/R^2\right)\pi d}. \tag{8}$$

Details on the derivation of (8) may be found in Appendix A. The distance model is summarized and depicted in Figure 2.

3. ENERGY CONSUMPTION ANALYSIS

According to the framework and definitions given in Section 2, the energy consumption in the cases of MIMO-based and multihop-based structures may be furtherly analyzed as follows.

3.1. Energy consumption of MIMO-based network

Using the energy and space models presented in Section 2 and assuming that $E_b^t = E_b^r = E_b(d_k, n)$ and $E_b^l = E_b(D, n)$, we derive

$$E_{\text{MIMO}} = L_{\text{MIMO}} M_t E_b(d,n)\left(1 + \frac{(M_r - 1)n_r}{b}\right) + L_{\text{MIMO}} M_t E_b(D,n). \tag{9}$$

Using (3) for $E_b(d,n)$ and $E_b(D,n)$, we evaluate the energy consumed for the transmission of L bits of data for a MIMO-based network according to

$$E_{\text{MIMO}} = \left(E_{f,1} + E_{f,2}E_{f,3\_\text{local}}d^n\frac{\alpha+1}{R_{b,\text{local}}} + E_{f,3\_\text{long-haul}}D^n\frac{\alpha+1}{R_{b,\text{long-haul}}}\right)L, \tag{10}$$

where $R_{b,\text{local}}$, $R_{b,\text{long-haul}}$ are the data rates (in bits per second) used in the local and the long-haul transmissions, respectively, estimated according to [3], and the factors $E_{f,i}$ are given by

$$\begin{aligned} E_{f,1} &= E_{f,2}E_{f,4} + \frac{(P_c + P_{\text{detector}})T_{\text{on,long-haul}} + 2P_{\text{syn}}T_{\text{tr}}}{L}, \\ E_{f,2} &= \left(1 + \frac{(M_r - 1)n_r}{b}\right), \\ E_{f,3\_j} &= \left(\frac{4\pi d_0}{\lambda}\right)^2 10^{((E_b/N_0)+R_{b,j}+S-204-G_t-G_r)/10}, \\ & \qquad j = \text{local, long-haul}, \\ E_{f,4} &= \frac{(P_c + P_{\text{detector}})T_{\text{on,local}} + 2P_{\text{syn}}T_{\text{tr}}}{L}, \end{aligned} \tag{11}$$

where $T_{\text{on,local}}$, $T_{\text{on,long-haul}}$ represent the time needed for the transmission of L bits according to the data rate. The variable d, that expresses the average transmission range of the nodes, depends on $\overline{d_k}$ and therefore ρ_s. From (10), it is obvious that the main factors affecting energy consumption are the path loss factor, the distance D between *source* and *destination nodes*, and the network's density ρ_s.

It should be clarified that in the long-haul transmissions, the average range is equal to D, which means that the M_t transmitting nodes are able to adjust their transmission power to achieve that specific average range. That is feasible if we assume that the *destination node* broadcasts a pilot symbol during the initial phase of the network's operation, using a globally known transmission power level $P_{t,\text{dest}}$. Each node can estimate the transmission power needed to reach the *destination* node using the knowledge of the path loss, which is derived by comparing the power level of the received signal, $P_{r,\text{dest}}$, to the transmission power level, as shown in the following equation:

$$PL = P_{t,\text{dest}} - P_{r,\text{dest}}. \tag{12}$$

It is also possible that the node with the role of the *destination* changes periodically. In that case, every time a *destination* node change happens, a pilot symbol has to be sent again from the new *destination* to notify the nodes of the network. Finally, considering local transmissions in MIMO structure, they are done assuming that each node is able to exchange data with its neighbor nodes ($\overline{d_n} = \overline{d_k}$).

3.2. Energy consumption of SISO multihop approach

When the network is based on the traditional multihop approach, then the total energy needed for the transmission of L bits is given by (1). The average number of hops, $\overline{H_{\text{multi}}}$, for a given distance D is

$$\overline{H_{\text{multi}}}(\overline{d_n}, D) = \frac{D}{\overline{d_n}} = \frac{D}{d - \overline{x}}. \tag{13}$$

Using this expression along with the energy model described by (3), we get the form of (14), describing the energy consumption during SISO multihop transmission:

$$\begin{aligned} E_{\text{multihop}} &= LE_b(d,n)\overline{H_{\text{multi}}}(\overline{d_n}, D) \\ &= \frac{E_{f,4} + E_{f,3\_\text{local}}d^n\left((\alpha+1)/R_{b,\text{local}}\right)}{\overline{d_n}}LD. \end{aligned} \tag{14}$$

Once again, the energy consumption depends on three main factors: the path loss factor n, the distance D, and the network density ρ_s, expressed via the distance $\overline{d_k}$. The total performance of such a multihop structure is straightforwardly dependant on the transmission power, P_t, and therefore the transmission range d. Hence, we will examine two different cases considering the value of d in the multihop operation. According to the first case, d is the range needed for the first neighbor node to be the *next hop*. Hence, $\overline{d_n} = \overline{d_k}$, and d is given by (7) that reduces to

$$d = \overline{d_k} + \overline{x}. \tag{15}$$

Alternatively, we utilize an optimization algorithm that estimates the value of P_t and hence d, and minimizes the total energy consumption on multihop-based networks, as it is expressed by (14). Minimizing that expression, for $n = 2$, we get

$$d = d_{\text{opt}} = \frac{\overline{d_k} + \sqrt{\overline{d_k}^2 + 4\left(E_{f,4}/\left(E_{f,3\_\text{local}}\left((\alpha+1)/R_{b,\text{local}}\right)\right)\right)}}{2}, \tag{16}$$

and $\overline{d_n}$ is estimated by (7). The transmission power used is defined according to

$$P_{t,\text{opt}} = P_t(d_{\text{opt}}, n). \tag{17}$$

For values of $n > 2$, the expressions of d_{opt} are more complicated and are computed numerically. More details regarding the optimization of the transmission power and average range for minimizing total energy consumption in multihop networks are given in [10]. We should mention that for very small values of D, the multihop optimization algorithm may result in worse performance than that of simple multihop approach. That is because these values of D actually refer to cases where the destination node is within the range of the source node, and thus only a single hop is needed for the data to be delivered.

Having estimated (10) and (14), the problem is defined as follows. Calculate the threshold values for the parameters n, ρ_s, D for which

$$E_{\text{MIMO}} < E_{\text{multihop}}. \tag{18}$$

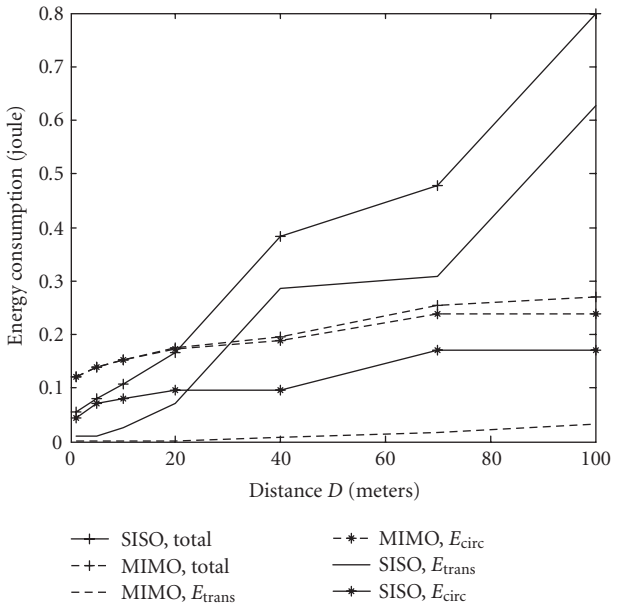

Figure 3: Energy consumption segregation for SISO and MIMO architectures versus distance.

Table 2: Indicative parameters value.

Bits to be transmitted (L)	10000
Frequency (f)	2500 (MHz)
n_r	10
M_t	2
M_r	2
Target bit error rate (BER)	10^{-5}
Antenna gains ($G_t \times G_r$)	5 dBi
S	10 dB
Reference distance (d_0)	0.5 m
R	50 m

3.3. Power dissipation analysis

Before proceeding with the analysis of (18), we focus on distinguishing the energy consumed by the circuitry of the node, denoted with E_{circ}, from the energy that depends on the transmission power, E_{trans}, based on the model presented in Section 2:

$$E_b = E_{trans} + E_{circ},$$
$$E_{trans} = \frac{(a+1)P_t T_{on}}{L}, \quad (19)$$
$$E_{circ} = \frac{(P_c + P_{detector})T_{on} + 2P_{syn}T_{tr}}{L}.$$

The importance of the power dissipated in the circuitry on the total performance of the MIMO architecture is obvious from Figure 3, which depicts the total energy consumption for MIMO 2×2 and SISO architectures versus the distance of the long-haul transmission, based on the parameters shown in Tables 1 and 2 and explained in detail in [9]. Distance in local transmissions is assumed to be fixed and equal to 1m, while the constellation sizes used are derived from the rate-optimization algorithms presented in [10]. According to that figure, a 2×2 MIMO structure is more energy-efficient than a SISO-based WSN when the distance between the receiver and the transmitter sides is greater than 20 m. We may observe though that the term that actually increases the energy consumption in the MIMO approach is E_{circ}, which includes the energy consumed by all electronics that do not have to do with transmission power, such as filters, mixers, and so on. If we consider the rapid deployment in microelectronics during the last years, then it is highly expected that more energy-efficient circuitry will be available soon. Therefore, MIMO structure is expected to become more energy-efficient. This is not the case with the SISO approach though, where E_{trans} inserts the greater parts of energy consumption. Less energy consumed in the circuitry results in lower distance thresholds and thus makes the MIMO structure more energy-efficient for almost any case.

Table 3: Examined scenarios.

Scenario 1	$E_{circ} = 10$ uJ
Scenario 2	$E_{circ} = 1$ uJ
Scenario 3	$E_{circ} = 0.1$ uJ

In order to examine the effect of E_{circ} on the distance thresholds above which the MIMO structure is more energy-efficient than SISO multihop transmission, we use three different scenarios for the value of E_{circ} as shown in Table 3. Scenario 1 corresponds to the values of Table 1. As shown in the next section, reducing E_{circ} results in remarkable changes regarding the threshold values that determine when MIMO-based structures are more energy-efficient.

4. THRESHOLDS ESTIMATION AND TENDENCIES

4.1. System analysis

In this section, we proceed with the estimation of the threshold values for the three crucial factors affecting the energy consumption, namely, the path loss factor n, the distance D, and the network density ρ_s. Indeed, we calculate the threshold values for which (18) is satisfied. We examine the performance of three different transmission structures. The first two are based on forwarding the data using H_{multi} multiple hops. That is, the source node sends the data to the destination node using several intermediate nodes, each of which receives and forwards the information. In the first structure (denoted as Multihop), the next hop at each transmission is chosen to be the closest node to the one that forwards the data. In the second structure (denoted as Multihop_opt), the next hop is chosen based on the optimization algorithm already described in Section 3. Finally, the third examined structure is based on a virtual 2×2 MIMO scheme. Both the source and the destination nodes choose one neighbor node to cooperate with and form virtual MIMO transmitter and receiver, respectively. The data is then sent using the Alamouti coding scheme. In this section, we assume that the cooperation node is chosen randomly among the neighbor

nodes, while in the next section a selection algorithm is proposed. For all examined schemes, we use a target BER value equal to 10^{-5}, while in the MAC layer we assume a simple slotted Aloha protocol. As far as the way the data is routed within the network to reach the destination node, we use an assumption commonly found in the literature, according to which information about the destination node is included into the data packets. For the figures that presented this point forward, the following configuration is assumed. Regarding the energy model, the values shown in Table 1 are used, while typical values for all other variables considering the evaluation of energy consumption are summarized in Table 2. For both local and long-haul transmissions, we assume Rayleigh fading channels. As far as the density is concerned, we consider a fixed deployment area with $R = 50$ m, while the total number of nodes, M, varies. According to the value of M, we get the node density from (5), measured in nodes per surface A (nodes/A). In our case, A is an area of 1 m^2, and the density may take values from 0.003 to 0.05, and thus the average distance between neighbor nodes varies between 2.2 and 9 m.

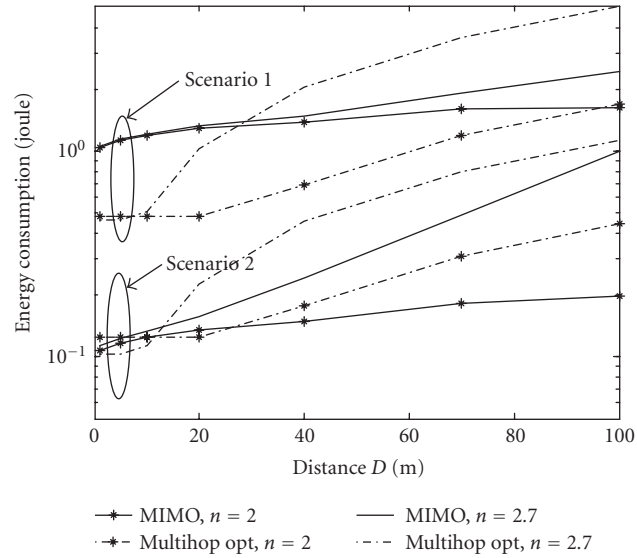

FIGURE 4: Total energy consumption versus D when $\rho_s = 0.01$ ($M = 100$) and $n = 2.0$, $n = 2.7$.

4.2. Interference issues

In wireless networks, and especially in networks with the characteristics of WSNs, a very important issue to be taken into consideration is interference. According to [15], the total interference at a node m and time k is given by

$$I_m[k] = \sum_{l=1}^{N_P} P_t \gamma_{lm}[k] + \sum_{j=1}^{D} P_t \gamma_{jm}[k], \tag{20}$$

assuming that the interference at each relay can be due to either other sources transmitting simultaneously or due to the other intermediate nodes which are in their transmission phase at time k and have started reception at time $k-1$. In (20), γ_{ij} is the channel gain between nodes i, j, D is the total number of interfering relays, and N_P is the number of sources at time k.

In our case though, where only two nodes cooperate to transmit data using the Alamouti coding, (20) includes one single factor as only one node transmits simultaneously with our source node. Hence, interference as expressed in (20) is limited. It is well understood [16] that the number of interferers clearly increases the interference problem in wireless networks. The fact that in our scenarios we only focus on cases where one interference node is present reduces the impact of such a problem.

Moreover, basic channel state knowledge, which is present in our scenarios, significantly affects the network's tolerance in interference [17]. In the same paper [17], the authors prove that the better the channel conditions are, the more tolerant the MIMO structures in interference will be.In particular, it is shown that unless the channel conditions are severe (e.g., $n = 3.5$), the effect of interference on MIMO structures' performance is negligible. As we analytically discuss in the next subsections, MIMO-based WSNs outperform multihop transmission schemes mainly in scenarios where the channel conditions are good. Hence, we may conclude that in such scenarios, which are of the main interest in this paper, interference can be assumed as negligible.

Finally, it has been stated in [18] that Alamouti-based transmission provides a very good performance in interference reduction. Hence, we focus on scenarios that use this specific simple space-time coding scheme, in order not to increase complexity as well as the interference effect.

4.3. Solving subject to the distance D

Solving inequality (18) for the distance between *source* and *destination nodes*,we get the polynomial expression

$$\left[E_{f,3\_\text{long-haul}} \frac{L(\alpha+1)}{R_{b,\text{long-haul}}}\right] D^n - \left[\frac{E_{f,4} + E_{f,3\_\text{local}} d^n \left((\alpha+1)/R_{b,\text{local}}\right)}{\overline{d_n}}\right] D + \left[E_{f,1} + E_{f,2} E_{f,3\_\text{local}} \overline{d_k}^n \frac{\alpha+1}{R_{b,\text{local}}}\right] > 0, \tag{21}$$

where $\overline{d_n}$ and d may take values according to two different cases, simple and optimized, as already explained in Section 3.2. A numerical solution algorithm for the polynomial is presented in Appendix B. In what follows, results will be presented based on the general form described by (21). Figure 4 depicts the total energy consumption for the case of a path loss factor equal to 2 or 2.7 and for a network consisting of 100 nodes, for the optimized multihop and the MIMO structures. If we assume $n = 2.0$ and current state of the art (scenario 1), using MIMO-based transmission results in more energy consumption for almost any value of D. The threshold values though seem to change significantly for scenario 2, where the MIMO structure is to be more energy-efficient for $D > 25$ m, a value that is also verified by the

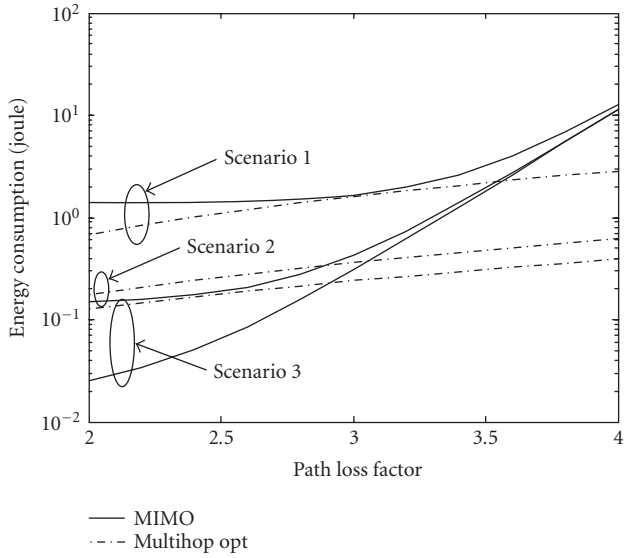

FIGURE 5: Total energy consumption versus n when $\rho_s = 0.01$ ($M = 100$) and $D = 40$ m.

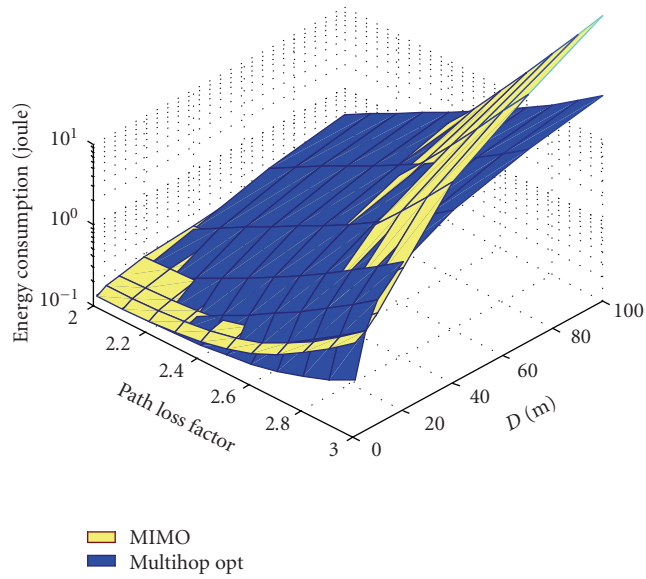

FIGURE 6: Total energy consumption versus n and D when $\rho_s = 0.01$ ($M = 100$).

numerical solution of (21) ($D_{\text{threshold,numerically}} \approx 24.21$ m). Using (6), we derive that $\overline{D} = 38.25$ m, and therefore the MIMO structure is expected to perform better than the simple multihop case for scenario 2. In the case of $n = 2.7$, we may reach a similar conclusion, as if scenario 2 is used instead of scenario 1, the threshold value above which the MIMO scheme outperforms optimized multihop transmission reduces from 30 to 10 m.

4.4. Solving subject to the path loss factor n

Inequality (18) leads us to the form of (22), when trying to solve it with respect to the path loss factor n:

$$\left[E_{f,3\_\text{long-haul}}\frac{L(\alpha+1)}{R_{b,\text{long-haul}}}\right]D^n - \left[\frac{E_{f,3\_\text{local}}\left((\alpha+1)/R_{b,\text{local}}\right)D}{\overline{d_n}}\right]d_n + \left[E_{f,2}E_{f,3\_\text{local}}\frac{\alpha+1}{R_{b,\text{local}}}\right]\overline{d_k}^{\,n} + \left[E_{f,1} - \frac{E_{f,4}D}{\overline{d_n}}\right] > 0. \tag{22}$$

Inequality (22) is n-grade exponential, and may be solved numerically according to the method described in Appendix C. The case of a network consisting of 100 nodes with $D = 40$ m is depicted in Figure 5. Although throughout the paper we mainly examine cases of $2 < n < 3$, in this first figure we expand the path loss factor's range to 4, in order to examine the performance for worse channel conditions. Regarding the 2nd scenario, for example, the threshold value below which the MIMO structure becomes more energy-efficient is $n < 2.8$. This value may also be verified numerically ($n_{\text{threshold,numerically}} \approx 2.77$). Similar threshold values may be extracted for the other two scenarios. Obviously, when the channel becomes much worse (e.g., $n > 3$), the energy consumption of the MIMO-based structure increases significantly. That is mainly due to the long-haul transmission, where the effect of the large values of n is greater. Hence, regarding the examined structures, energy gains may be feasible by MIMO schemes mainly for path loss factor values up to 3, as the threshold values mainly appear for the cases of $2 < n < 3$.

A more thorough view of the interrelation between the values of path loss factor and the distance between *source* and *destination nodes* is shown in Figure 6. We examine the case of a network consisting of 100 nodes, and the comparison is made between the MIMO and the optimized multihop scenarios for the 2nd scenario. We therefore conclude that multihop structure is more energy-efficient for the cases where D and n are both large, for example, $n > 2.7$ and $D > 50$. There is also a small area where multihop outperforms MIMO if $D < 10$ and $n < 2.4$.

4.5. Solving subject to network density ρ_s

The last variable examined regarding the effect on energy efficiency of MIMO-based sensor networks is the node density ρ_s. Density is expressed through the average distance between two neighbor nodes, $\overline{d_k}$, and inequality (18) takes a form that depends on the multihop scenario examined. If the transmission range is set according to (15), then the inequality to be solved is the polynomial

$$\left[E_{f,2}E_{f,3\_\text{local}}\frac{\alpha+1}{R_{b,\text{local}}}\right]\overline{d_k}^{\,n} - \left[E_{f,3\_\text{local}}2^n\frac{\alpha+1}{R_{b,\text{local}}}\right]\overline{d_k}^{\,n-1} - DE_{f,4}\overline{d_k}^{\,-1} + \left[E_{f,3\_\text{long-haul}}D^n\frac{L(\alpha+1)}{R_{b,\text{long-haul}}} + E_{f,1}\right] > 0. \tag{23}$$

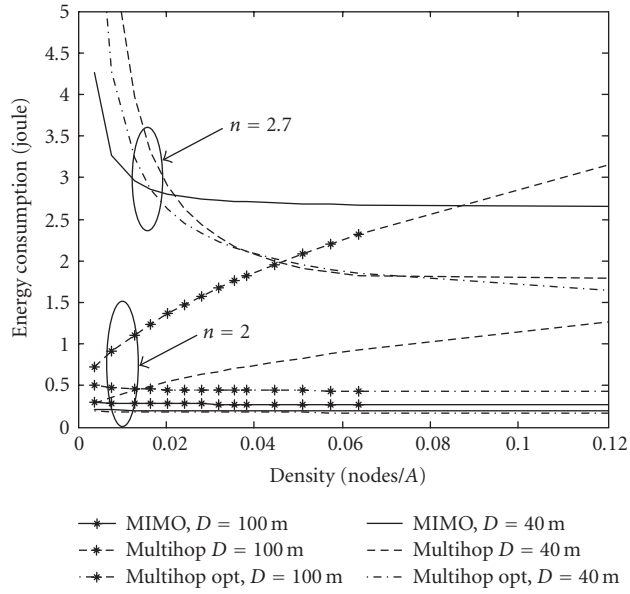

Figure 7: Total energy consumption versus density when $n = 2$ and $D = 40$, $D = 100$.

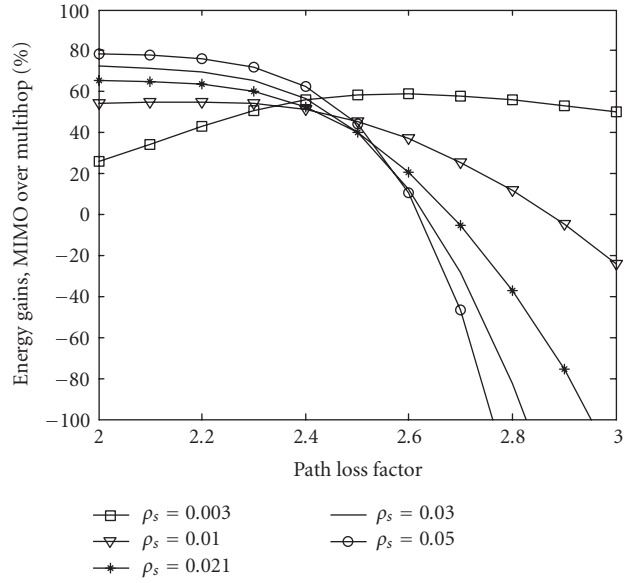

Figure 8: Energy gains inserted for $D = 40$ m and different network densities.

This equation may as well be solved numerically using the method described in Appendix B. When the optimization algorithm is used and transmission range is set according to (16), then we get the form of inequality (24) derived for the simple case of $n = 2$:

$$\left[E_{f,2}E_{f,3\_\text{local}}\frac{\alpha+1}{R_{b,\text{local}}}\right]\overline{d_k}^2 - \left[E_{f,3\_\text{local}}\frac{\alpha+1}{R_{b,\text{local}}}\right] \times \frac{\left(\overline{d_k}+\sqrt{\overline{d_k}^2+4\left(E_{f,4}/E_{f,3\_\text{local}}\left((\alpha+1)/R_{b,\text{local}}\right)\right)}\right)^2}{\overline{d_k}2^2} - DE_{f,4}\overline{d_k}^{-1} + \left[E_{f,3\_\text{long-haul}}D^2\frac{L(\alpha+1)}{R_{b,\text{long-haul}}}+E_{f,1}\right] > 0. \quad (24)$$

Having clarified the effect of potential reduction of E_{circ} on the MIMO structure's performance, in this paragraph we restrict our investigation to scenario 2 and we focus on the interrelation between D, n, and ρ_s. The energy consumption for the three examined schemes is depicted in Figure 7 for the cases of $n = 2$ or 2.7 and $D = 40$ m, $D = 100$ m. Let us first examine the case of $n = 2$. As one observes for $D = 40$ m, increasing the density mainly affects the first case of multihop structure. MIMO structure, on the other hand, performs slightly worse than optimized multihop for all densities. If we increase the distance D to 100 m, the MIMO-based network is less affected, and hence it becomes more energy-efficient than both multihop schemes. The simple multihop structure is still highly affected by the density, and its performance gets worse as the density increases. This was anticipated since in this case the next hop is the closest node in the network, and therefore increasing the density increases the number of hops. On the other hand, when the optimized distance is used, the energy consumption slightly decreases with the increase of the density up to a point beyond which the dominant factor in (16) is no more the distance $\overline{d_k}$ but rather the rest terms that are fixed.

Increasing the path loss factor to 2.7 though significantly changes the interrelation between density and energy consumption. Now, the performance of all schemes in terms of energy efficiency improves as the density increases. The improvement is more rapid in the multihop schemes, and thus there is an upper threshold in the density below which the MIMO-based network is more energy-efficient.

Figure 8 gives an overview of the gains inserted due to MIMO structure with respect to the simple multihop case, for several network densities, and for $D = 40$ m. In general, when the channel is good, the MIMO-based scheme offers remarkable gains in terms of total energy consumption. The gains become greater as the network density increases. On the other hand, when $n > 2.5$, sparser networks offer greater gains for the MIMO case. Depending on the density, there is a critical value of n above which the multihop scheme becomes more energy-efficient.

4.6. Performance regarding time delay

Apart from energy efficiency, a critical issue regarding the performance in WSNs is the time delays inserted until the data arrives at the destination node. Hence, it is important to investigate the effect of the MIMO-based structure on the time delay with respect to simple multihop transmission.

Assuming that the data is transmitted using multiple hops,then the time needed for the data to be delivered to the destination node is

$$T_{\text{multihop}} = H_{\text{multi}}t_{\text{local}}, \quad (25)$$

where t_{local} is the time needed for the data to be transmitted from one node to the next hop node.

On the other hand, for 2×2 MIMO-based structures, the time delay may be expressed as follows:

$$T_{\text{MIMO}} = 2t_{\text{long-haul}} + t_{\text{add}}, \tag{26}$$

where $t_{\text{long-haul}}, t_{\text{add}}$ are the time delays for the long-haul transmission and for the additional symbols that are needed to be exchanged for the formation of the virtual MIMO transceivers, respectively. Using the Alamouti coding scheme, 2 long-haul time slots are needed for the data to be delivered.

The data rates used in local and long-haul transmissions are the same; so we assume that

$$t_{\text{local}} = t_{\text{long-haul}} = T_{\text{on}}, \tag{27}$$

where T_{on}, as defined earlier, is the time needed for the packet of data to be transmitted from one node to another. Moreover, regarding t_{add}, it includes the time spent for the pilot symbols needed to form the virtual MIMO transceiver as well as the time needed for the actual data to be exchanged, both at the transmitter's side and the receiver's side. At the transmitter's side, the essential transmission is the one between the first node that senses the data and the node chosen for cooperation. At the receiver's side, data has to be sent to the destination node from the node chosen for cooperation. Therefore, $2T_{\text{on}}$ is required for actual data transmissions. Having the cooperation node chosen randomly among neighbors and using only 2×2 systems, we conclude that one pilot symbol is enough for the transceiver's formation and the time delay inserted is negligible. Hence,

$$t_{\text{add}} = 2T_{\text{on}}. \tag{28}$$

Combining the above, we may derive

$$\begin{aligned} T_{\text{multihop}} &= H_{\text{multi}}T_{\text{on}}, \\ T_{\text{MIMO}} &\simeq 4T_{\text{on}}. \end{aligned} \tag{29}$$

According to the scenarios examined in this paper, we derive from (13) that H_{multi} may vary from 4 up to 18. Therefore, we may conclude that using 2×2 MIMO-based structures does not insert any additional time delays.

However, assume that t_{add} takes greater values than $2T_{\text{on}}$. It is clear from (29) that depending on the value of H_{multi}, T_{MIMO} may be still less than T_{multihop} for values of t_{add} up to $8T_{\text{on}}$. Of course there are some cases where MIMO-based structure may insert greater time delays than multihop scenarios, but this requires that t_{add} be significantly higher than estimated.

5. THRESHOLD ESTIMATION AND COOPERATIVE NODE SELECTION ALGORITHM

In this section, we implement a simple cooperative node selection algorithm in the 2×2 MIMO structure, to achieve enhanced energy efficiency. The algorithm's implementation affects the threshold values estimated in this section. We will investigate these effects and re-examine the interrelations between the critical variables already mentioned.

5.1. The cooperative node selection algorithm

We implement a simple cooperative node selection algorithm based on estimations of the channel conditions in the links between neighboring nodes. This algorithm applies to MIMO structures described in previous sections. We introduce a novel metric TEL (total energy lifetime), that is defined as follows.

Assume that the channel in both local and long-haul transmissions suffers from log-normal shadowing and that each node has to choose among N neighbor nodes for cooperation. That is, the received power at each node j ($j = 1, 2, \ldots, N$) after a source node transmits a packet of datais estimated by

$$\begin{aligned} P_r^j &= P_t - PL(d_j) + G_t + G_r \\ &= P_t - \overline{PL(d_j)} - \chi + G_t + G_r, \end{aligned} \tag{30}$$

where G_t, G_r are the gains of the transmitter and receiver antennas, respectively, and henceforth they are set to 0 dBi. All factors are expressed in logarithmic scale. Shadowing is expressed by the normally distributed variable χ, with zero mean and variance equal to 5 dB. If we assume that at the beginning of the network's operation each node sends a pilot symbol and waits for acknowledgments to specify its neighbors, then the knowledge of the transmission power level combined with the knowledge of the acknowledgement's power level allows the node to be aware of the path loss given by (30). As the path loss values experienced by the links greatly affect the total energy consumed in the network, TEL is a function of $PL(d_j)$: $\text{TEL}_j = f(PL(d_j))$.

Apart from the total energy consumed in the network, another important metric to measure energy efficiency is lifetime. When energy is uniformly consumed within the network, increased lifetime is assured. Therefore, TEL also includes information about the energy left at each node j, denoted with E_{left}^j: $\text{TEL}_j = f(E_{\text{left}}^j)$.

The cooperation node (CN) is selected according to

$$\begin{aligned} \text{TEL}_j &= \frac{PL(d_j)}{E_{\text{left}}^j}, \\ \text{CN} &= \arg\min\{\text{TEL}_j\}. \end{aligned} \tag{31}$$

The CN selection is made by the source node as well as the destination node, at the transmitter and receiver sides, respectively. In our case, only 2×2 systems are examined, and hence both source and destination nodes will choose only one node to cooperate with. Since the selection is based on both the channel state and the energy left at each neighbor, the optimum CN is re-estimated every time a node has data to retransmit. Upon selection, the CNs at the transmitter and receiver sides are informed by the source or the destination node, respectively.

5.2. Effect of CN selection on general performance

Before proceeding with the effect of the CN selection algorithm on the threshold values, we examine the general

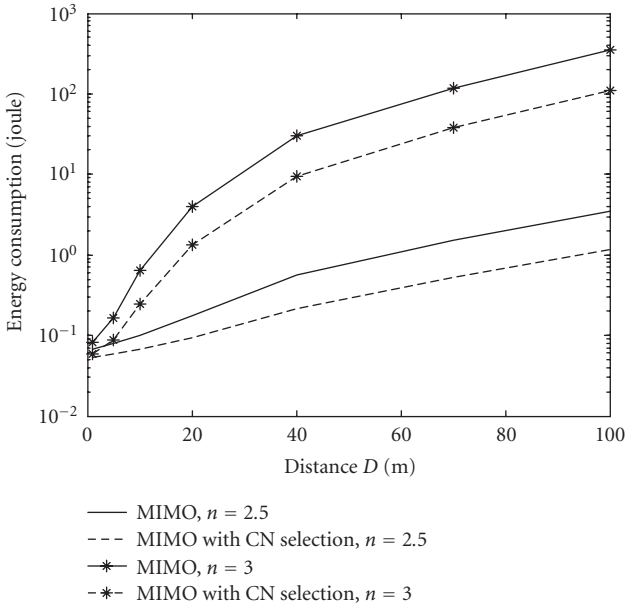

Figure 9: Effect of CN algorithm on total energy consumption, $M = 100$.

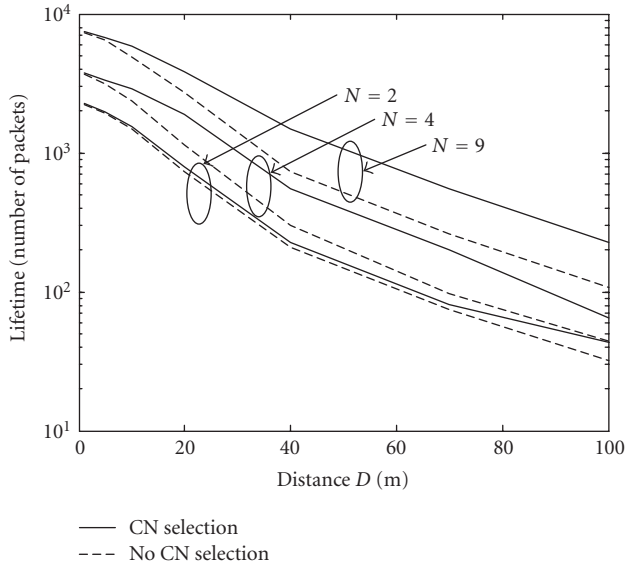

Figure 10: Effect of CN algorithm on network's lifetime; $n = 2.5$, $M = 100$.

performance of a MIMO-based WSN using the proposed scheme. The implementation of the specific algorithm in our networks requires the transmission of some additional pilot messages. The fact that we consider only 2×2 systems results in the additional energy consumption being much less than the energy needed for the actual data transmission. Nevertheless, that energy cost has been taken into account in the following. In Figure 9, we observe the total energy consumption in a network consisting of 100 nodes for two different cases regarding the path loss factor. It is obvious that the gains inserted due to CN selection become remarkably greater as the channel conditions get worse. For the case of $n = 2.5$, energy gains are close to 100% for a distance equal to 25 m.

As already stated, the implemented CN algorithm also focuses on increasing the network's lifetime by distributing uniformly the energy consumption within the network. This is also depicted in Figure 10, for a network consisting of 100 nodes and $n = 2.5$. Here, lifetime is defined as the number of packets delivered until the first node runs out of energy. The algorithm's effect on the lifetime depends on the number of possible neighbors N from which the source node has to choose the CN, as more neighbors result in more uniformly distributed energy consumption. Hence, we examine three different cases regarding N. One observes that even when the choice is made out of two nodes, gains are inserted in terms of lifetime. As the number of neighbor nodes increases, the gains become greater. The decreased lifetime observed when fewer nodes are used in the transmitter's side is due to the fact that fewer nodes are used to transmit the same amount of data, and hence they remain out of energy faster.

The implementation of such an algorithm may also affect the time delays until the data is delivered to the destination node. Both the source and the destination nodes now search among all their neighbors in order to find the best one to cooperate with. On the other hand, the actual data will be transmitted only once between cooperation nodes, just as in the simple case described in Section 4.6, after the CN selection has been made. Hence, the additional time delays are due to the time needed for the completion of the CN selection ($t_{\text{CN\_selection}}$), which includes only pilot symbols:

$$t_{\text{add}} = 2T_{\text{on}} + t_{\text{CN\_selection}}. \tag{32}$$

The value of $t_{\text{CN\_selection}}$ depends on the number of pilot symbols needed for the cooperation node to be chosen, and consequently on the number of neighbors of both the source and destination nodes. Having in mind though that the time needed for a pilot symbol is much less than the delays inserted by sending the actual data and knowing that in general the MIMO-based structure inserts less time delays than the multihop transmission based on (29), we conclude that the CN selection algorithm does not affect the system's performance in terms of total time delays.

5.3. Effect of CN selection on threshold values

Figure 11 summarizes the node selection algorithm effect on the threshold values D for the case of $n = 2.7$. When the node density is small ($\rho_s = 0.003$), the MIMO-based network seems to operate more energy-efficiently than the multihop-based network for any value of $D > 31$ m. This threshold value drops to 25 m, when the CN selection algorithm is used. Increasing network's density decreases the threshold values of D that determine the critical points for the MIMO structure, but the improvement inserted due to CN selection remains remarkable.

An overall view of the threshold values change due to CN selection implementation is given by Figure 12 for a network consisting of 100 nodes. A comparison with Figure 6 clarifies the gains inserted by the CN selection algorithm. The MIMO

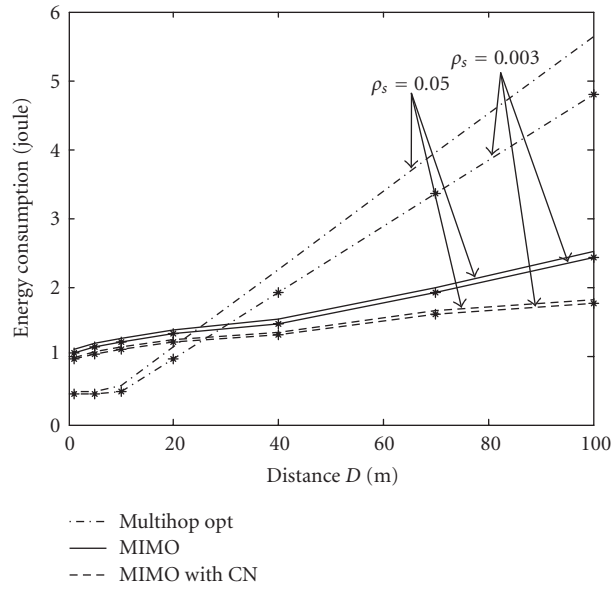

FIGURE 11: Effect of node selection algorithm on thresholds estimations when $n = 2.7$ and ($\rho_s = 0.003$) ($M = 30$), ($\rho_s = 0.05$) ($M = 500$).

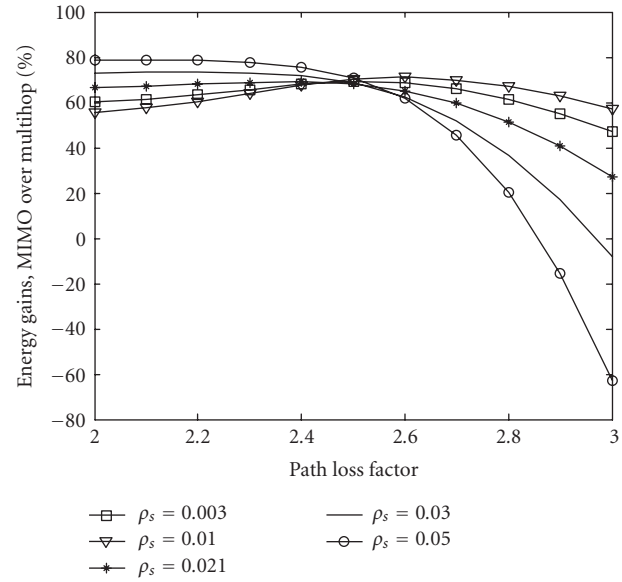

FIGURE 13: Energy gains inserted with CN selection for $D = 40$ m and different network densities.

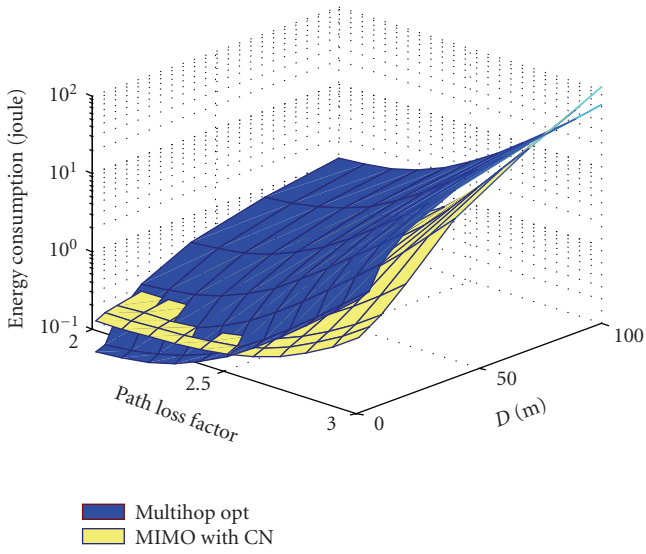

FIGURE 12: Total energy consumption when CN selection is used versus n and D when $\rho_s = 0.0127$ ($M = 100$).

structure now outperforms the optimized multihop scheme for almost any examined case regarding path loss factor and distance D.

Finally, Figure 13 provides the total energy gains inserted when MIMO structure is used in combination with CN selection, with reference to the case of multihop transmission. The depicted results are for $D = 40$ m and show that the energy gains are remarkable for most of the combinations of the network density and the path loss factor. Moreover, we compare the gains with the ones provided by the simple MIMO case in Figure 8, and we observe that, especially for $2.2 < n < 2.8$ and for low densities, the additional gains inserted are greater than 20%.

6. CONCLUSIONS

During the last few years, MIMO structures have been proposed in sensor networks to improve the performance in terms of energy efficiency, compared to the simple SISO case. In this paper, we extended this research by examining the energy efficiency of MIMO-based sensor networks in comparison to two alternative SISO multihop approaches. We reached expressions to estimate threshold values regarding the channel conditions, the distance between *source* and *destination nodes,* and the network density, which determine the areas where the MIMO structure is more energy-efficient. Moreover, we considered future tendencies in technology evolution and combined the above results with different scenarios regarding the hardware electronics as well as with the implementation of a simple cooperative node selection algorithm. Summarizing the main conclusions, for realistic channel conditions (e.g., $n = 2.7$), the sparser the network is, the more the cases where MIMO-based networks are more energy-efficient will be. In addition, as the path loss factor reaches lower values, the gains inserted due to the MIMO approach increase. On the other hand, if the channel is bad, the multihop approach becomes more energy-efficient, and the greater the network density is, the more the gains inserted due to multihop transmission are. All these thresholds become looser when we assume more energy-efficient electronics in the hardware—something which is highly expected in the short future. Finally, the results were also affected by the CN selection algorithm. Gains over 20% are expected according to the several conditions examined. Therefore, the thresholds that determine when MIMO-based networks outperform multihop structures become significantly looser.

APPENDICES

A. ESTIMATING $E[x]$

If d is the range of the node, then the probability of having a node in an area between $d-x$ and $d+x$, where $x \in (0, \overline{d_k})$, is given by

$$P_r(\text{node exists in area}) = \frac{\pi\left[(d+x)^2-(d-x)^2\right]}{4R^2}. \quad (A.1)$$

Then, the probability of no node being in the same area is given by

$$P_r(X > x) = \left[1 - \frac{\pi\left[(d+x)^2-(d-x)^2\right]}{4R^2}\right]^M \quad (A.2)$$

and the relative c.d.f. is therefore

$$\text{c.d.f.} = 1 - P(X > x) = 1 - \left[1 - \frac{\pi\left[(d+x)^2-(d-x)^2\right]}{4R^2}\right]^M. \quad (A.3)$$

From the c.d.f., we may straightforwardly compute the p.d.f. as

$$\text{p.d.f.} = \frac{M\pi d}{R^2}\left[1 - \frac{\pi\left[(d+x)^2-(d-x)^2\right]}{4R^2}\right]^{M-1}. \quad (A.4)$$

The mean value of the variable x is then estimated as follows:

$$E[x] = \overline{x} = \int_0^{\overline{d_k}} \text{PDF}\cdot x\,dx = -\overline{d_k}A^M + B\left(1 - A^{M+1}\right), \quad (A.5)$$

where the factors A, B are given by

$$A = \frac{R^2 - \pi d\overline{d_k}}{R^2}, \qquad B = \frac{1}{(M+1)(\pi d/R^2)}. \quad (A.6)$$

As $A < 1$, $\lim_{M\to\infty} A^M = 0$. In this paper, we examine scenarios with $M \geq 30$, which allows us to assume that $A^M \approx 0$ and thus all factors except B are equal to zero. Then, the above expression reduces to

$$E[x] \approx \frac{1}{(M+1)(\pi d/R^2)} = \frac{1}{(4\rho_s + 1/R^2)\pi d}. \quad (A.7)$$

B. NUMERICAL SOLUTIONS FOR POLYNOMIALS

The nth-grade polynomials, that appear in the cases of solving them versus D and $\overline{d_k}$, should be converted to integer-grade polynomials. Assuming that n takes discrete values in [2.0 3.0] with step equal to 0.1, we use the substitutions $y_1 = D^{1/10}$, $y_2 = \overline{d_k}^{1/10}$. Then, (21) and (23) take the form of

$$\begin{aligned} &A_1 y_1^{a_1} + B_1 y_1^{10} + K_1 > 0, \\ &A_2 y_2^{a_2} + B_2 y_2^{a_2-1} + C_2 y_2^{10} + K_2 > 0, \end{aligned} \quad (B.1)$$

where $a_1 = 10n$, $a_2 = 10(n+1)$ are integers and

$$\begin{aligned} A_1 &= E_{f,3\_\text{long-haul}}\frac{L(\alpha+1)}{R_{b,\text{long-haul}}}, \\ A_2 &= E_{f,2}E_{f,3\_\text{local}}\frac{\alpha+1}{R_{b,\text{local}}}, \\ B_1 &= \frac{E_{f,4} + E_{f,3\_\text{local}}d^n\left((\alpha+1)/R_{b,\text{local}}\right)}{\overline{d_n}}, \\ B_2 &= E_{f,3\_\text{local}}2^n\frac{\alpha+1}{R_{b,\text{local}}}, \\ K_1 &= E_{f,1} + E_{f,2}E_{f,3\_\text{local}}\overline{d_k}^n\frac{\alpha+1}{R_{b,\text{local}}}, \\ C_2 &= E_{f,3\_\text{long-haul}}D^n\frac{L(\alpha+1)}{R_{b,\text{long-haul}}} + E_{f,1}, \\ K_2 &= DE_{f,4}. \end{aligned} \quad (B.2)$$

Finally, we estimate its *companion matrices* C_{m1}, C_{m2} as

$$C_{m1} = \begin{bmatrix} 0 & 0 & \cdot & \cdot & c_0 = -\dfrac{K_1}{A_1} \\ 1 & 0 & \cdot & \cdot & 0 \\ 0 & 1 & 0 & \cdot & \cdot \\ \cdot & 0 & 1 & \cdot & c_{10} = -\dfrac{B_1}{A_1} \\ \cdot & \cdot & \cdot & \cdot & \cdot \\ 0 & 0 & \cdot & \cdot & c_{a_1-1} = 0 \end{bmatrix},$$

$$C_{m2} = \begin{bmatrix} 0 & 0 & \cdot & \cdot & c_0 = -\dfrac{K_2}{A_2} \\ 1 & 0 & \cdot & \cdot & 0 \\ 0 & 1 & 0 & \cdot & \cdot \\ \cdot & 0 & 1 & \cdot & c_{10} = -\dfrac{C_2}{A_2} \\ \cdot & \cdot & \cdot & \cdot & \cdot \\ 0 & 0 & \cdot & \cdot & c_{a_2-1} = -\dfrac{B_2}{A_2} \end{bmatrix}. \quad (B.3)$$

The solutions of the polynomials may then be estimated by calculating the eigenvalues of C_{m1}, C_{m2}, from which D and $\overline{d_k}$ may be easily extracted.

C. SOLVING THE EXPONENTIAL EQUATION

In order to solve the exponential equation, we will first turn it into a polynomial one, and then use the method described in Appendix B. The problem to be solved is described by

$$aA^n - bB^n + cC^n + d = 0, \quad (C.1)$$

where

$$a = \left[E_{f,3\_\text{long-haul}} \frac{L(\alpha+1)}{R_{b,\text{long-haul}}} \right],$$

$$b = \left[\frac{E_{f,3\_\text{local}}((\alpha+1)/R_{b,\text{local}})D}{\overline{d_n}} \right],$$

$$c = \left[E_{f,2} E_{f,3\_\text{local}} \frac{\alpha+1}{R_{b,\text{local}}} \right], \tag{C.2}$$

$$d = \left[E_{f,1} \frac{E_{f,4} D}{\overline{d_n}} \right],$$

$$A = D, \qquad B = d, \qquad C = \overline{d_k}.$$

We use the following transformation set:

$$X = A^n, \qquad Y = B^n, \qquad Z = C^n \tag{C.3}$$

from which, using logarithms, we get

$$X = Y^K, \quad K = \frac{\ln A}{\ln B},$$
$$Z = Y^L, \quad L = \frac{\ln C}{\ln B}. \tag{C.4}$$

Equations (C.3) and (C.1) lead to

$$aX - bY + cZ + d = 0 \tag{C.5}$$

which, with the help of (C.4), results in the polynomial

$$aY^K - bY + cY^L + d = 0. \tag{C.6}$$

Equation (C.6) may then be solved using the method described in Appendix B.

ACKNOWLEDGMENT

This work has been done within the framework of the project PENED 2003 entitled "Data transmission techniques in Wireless Sensor Networks", partially funded by the European Union.

REFERENCES

[1] I. F. Akyildiz, W. Su, Y. Sankarasubramaniam, and E. Cayirci, "A survey on sensor networks," IEEE Communications Magazine , vol. 40, no. 8, pp. 102–114, 2002.

[2] G. J. Foschini and M. J. Gans, "On limits of wireless communications in a fading environment when using multiple antennas," Wireless Personal Communications , vol. 6, no. 3, pp. 311–335, 1998.

[3] S. Cui, A. J. Goldsmith, and A. Bahai, "Energy-efficiency of MIMO and cooperative MIMO techniques in sensor networks," IEEE Journal on Selected Areas in Communications , vol. 22, no. 6, pp. 1089–1098, 2004.

[4] S. K. Jayaweera, "Energy analysis of MIMO techniques in wireless sensor networks," in *Proceedings of the 38th Annual Conference on Information Sciences and Systems (CISS '04)*, Princeton, NJ, USA, March 2004.

[5] L. Xiao and M. Xiao, "A new energy-efficient MIMO-sensor network architecture M-SENMA," in *Proceedings of the 60th IEEE Vehicular Technology Conference (VTC '04)*, vol. 4, pp. 2941–2945, Los Angeles, Calif, USA, September 2004.

[6] Y. Yuan, Z. He, and M. Chen, "Virtual MIMO-based cross-layer design for wireless sensor networks," IEEE Transactions on Vehicular Technology , vol. 55, no. 3, pp. 856–864, 2006.

[7] R. Lin and A. P. Petropulu, "A new wireless network medium access protocol based on cooperation," IEEE Transactions on Signal Processing , vol. 53, no. 12, pp. 4675–4684, 2005.

[8] A. Bletsas, A. Khisti, D. P. Reed, and A. Lippman, "A simple cooperative diversity method based on network path selection," IEEE Journal on Selected Areas in Communications , vol. 24, no. 3, pp. 659–672, 2006.

[9] G. Bravos and A. G. Kanatas, "Energy consumption and trade-offs on wireless sensor networks," in *Proceedings of the 16th IEEE International Symposium on Personal, Indoor and Mobile Radio Communications (PIMRC '05)*, vol. 2, pp. 1279–1283, Berlin, Germany, September 2005.

[10] S. Cui, A. J. Goldsmith, and A. Bahai, "Energy-constrained modulation optimization," IEEE Transactions on Wireless Communications , vol. 4, no. 5, pp. 2349–2360, 2005.

[11] B. Sklar, Digital Communications: Fundamentals and Applications , Prentice-Hall PTR, Upper Saddle River, NJ, USA, 2nd edition, 2001.

[12] M. K. Simon and M.-S. Alouini, Digital Communication over Fading Channels: A Unified Approach to Performance Analysis , Wiley-Interscience, New York, NY, USA, 2000.

[13] O. K. Tonguz and G. Ferrari, Ad Hoc Wireless Networks: A Communication-Theoretic Perspective , John Wiley & Sons, New York, NY, USA, 1st edition, 2006.

[14] S. Panichpapiboon, G. Ferrari, and O. K. Tonguz, "Sensor networks with random versus uniform topology: MAC and interference considerations," in *Proceedings of the 59th IEEE Vehicular Technology Conference (VTC '04)*, vol. 4, pp. 2111–2115, Milan, Italy, May 2004.

[15] S. Vakil and B. Liang, "Balancing cooperation and interference in wireless sensor networks," in *Proceedings of the 3rd Annual IEEE Communications Society on Sensor and Ad Hoc Communications and Networks (SECON '06)*, vol. 1, pp. 198–206, Reston, Va, USA, September 2006.

[16] K. Jain, J. Padhye, V. N. Padmanabhan, and L. Qiu, "Impact of interference on multi-hop wireless network performance," in *Proceedings of the 9th Annual International Conference on Mobile Computing and Networking (MobiCom '03)*, pp. 66–80, San Diego, Calif, USA, September 2003.

[17] A. M. Abbosh and D. Thiel, "Performance of MIMO-based wireless sensor networks with cochannel interference," in *Proceedings of the 2nd International Conference on Intelligent Sensors, Sensor Networks and Information Processing Conference (ISSNIP '05)*, pp. 115–119, Melbourne, Australia, December 2005.

[18] S. M. Alamouti, "A simple transmit diversity technique for wireless communications," IEEE Journal on Selected Areas in Communications , vol. 16, no. 8, pp. 1451–1458, 1998.